Journal of Applied Polymer Science

Characterization of 3D elastic porous polydimethylsiloxane (PDMS) cell scaffolds fabricated by VARTM and particle leaching

Junhui Si,[1,2] Zhixiang Cui,[2] Peng Xie,[2] Lairui Song,[3] Qianting Wang,[2] Qiong Liu,[2] Chuntai Liu[1]

[1]School of Materials Science and Engineering, Zhengzhou University, Henan 450001, China
[2]School of Materials Science and Engineering, Fujian University of Technology, Fujian 350118, China
[3]School of Materials Science and Engineering, Fuzhou University, Fujian 350000, China
Correspondence to: Z. Cui (E-mail: cuizhixiang2006@126.com) and C. Liu (E-mail: ctliu@zzu.edu.cn)

ABSTRACT: In this study, elastic porous polydimethylsiloxane (PDMS) cell scaffolds were fabricated by vacuum-assisted resin transfer moulding (VARTM) and particle leaching technologies. To control the porous morphology and porosity, different processing parameters, such as compression load, compression time, and NaCl particle size for preparing NaCl preform, were studied. The porous structures of PDMS cell scaffolds were characterized by scanning electron microscopy (SEM). The properties of PDMS cell scaffolds, including porosity, water absorption, interconnectivity, compression modulus, and compression strength were also investigated. The results showed that after the porogen–NaCl particles had been leached, the remaining pores had the sizes of 150–300, 300–450, and 450–600 μm, which matched the sizes of the NaCl particles. The interconnectivity of PDMS cell scaffolds increases with an increase in the size of NaCl particles. It was also found that the smaller the size of the NaCl particles, the higher the porosity and water absorption of PDMS cell scaffolds. The content of residual NaCl in PDMS/NaCl scaffolds reduces under ultrasonic treatment. In addition, PDMS scaffolds with a pore size of 300–450 μm have better mechanical properties compared to those with pore sizes of 150–300 and 450–600 μm. © 2015 Wiley Periodicals, Inc. J. Appl. Polym. Sci. **2016**, *133*, 42909.

KEYWORDS: biomedical applications; manufacturing; porous materials; structure–property relations

Received 26 May 2015; accepted 2 September 2015
DOI: 10.1002/app.42909

INTRODUCTION

In recent years, using various engineering tissue scaffolds for cell culture has drawn an increasing amount of attention in tissue engineering, regenerative medicine, biomedical engineering, and biological applications. For example, the cell culture *in vitro* model is the main experimental method used in cell biological research.[1] In general, cell scaffold, when serving as an artificial extracellular matrix, needs to provide a viable micro-environment for cell attachment, infiltration, proliferation, and differentiation, and serves as a template for cells to form new tissues.[2] Ideally, scaffolds for cell culture should be inherently biocompatible and have high porosity and interconnectivity for cell growth and flow transport of oxygen, nutrients, and excretion of metabolic waste.[3] Cells isolated or cultured on two-dimensional (2D) substrates cannot grow into functional three-dimensional (3D) cell constructs that are similar to native tissues. Therefore, the scaffolds with a 3D structure would be favored since they could afford cells a 3D growth environment by enhancing cell–cell contact, promoting the spatial arrangement of cells, and supporting high cell densities due to their high surface area-to-volume ratios. However, fabricating 3D highly porous scaffolds is still a challenge.

Polydimethylsiloxane (PDMS) is a synthetic polymer whose backbone is a repeating chain of Si—O molecules with two methyl groups attached to silicon atoms. PDMS has now been widely used in various fields, such as: biology, medical device implants, and regenerative medicine due to its excellent properties, such as it being inert, non-cytotoxic, and biocompatible.[4,5] Some special characteristics of PDMS, such as gas permeability, optical transparency, and flexibility also make it a good candidate for scaffold material to study cellular behavior and to investigate the effects of mechanical simulation on the biological behavior of cells.[6] For decades, dishes, flasks, and well-plates, with a 2D structure made by PDMS, have been widely used for cell culture. While, a major limitation on the use of these scaffolds is that cells only could be cultured on their 2D structure surface in monolayers.

Vacuum-assisted resin transfer moulding (VARTM) is one of the most fascinating methods for fibre-reinforced composite manufacture.[7] The advantages of VARTM include the simplicity of the method, low cost, its fast processing speed, and its moulding ability at room temperature.[8] Over the past two decades, VARTM has been widely used in the automobile, marine,

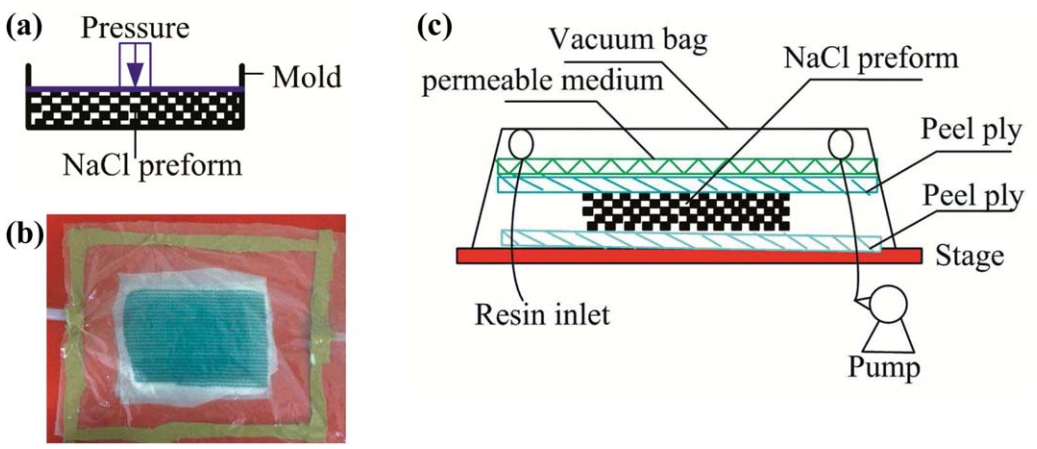

Figure 1. The process of manufacturing PDMS cell scaffolds. (a) The set-up for pre-forming NaCl; (b) Actual set-up of VARTM process; (c) Schematic illustration of VARTM process. [Color figure can be viewed in the online issue, which is available at wileyonlinelibrary.com.]

aerospace, and construction industries. Much research has been conducted on the resin infusion process in VATRM.[9,10] However, to the best of our knowledge, this technique has never been applied to cell scaffold fabrication. A VARTM technique would be an ideal manufacturing process to create 3D cell scaffolds due to its advantages of the simplicity of the devices used, ease of operation, low-cost manufacturing, repeatability, and formability of complex scaffolds. Moreover, a scaffold fabricated by the VARTM process would be highly porous with good pore-interconnectivity. Therefore, VARTM could be developed as a high-efficiency method of cell scaffold fabrication.

Based on the advantages of VARTM technology and PDMS as a material, this study aimed to fabricate a 3D porous PDMS scaffold with high porosity and interconnectivity for cell culture research. In this article, three different compression loads, compression times, and NaCl particle sizes were chosen to study the effect of processing parameters and porogen size on the properties of PDMS scaffolds. The morphologies, porosity, water absorption, interconnectivity, surface wettability, and mechanical properties of PDMS scaffolds were studied. Finally, the morphology and proliferation of osteoblasts from infant SD rats seeded on PDMS cell scaffolds were investigated.

MATERIALS AND METHODS

Materials

The liquid PDMS precursor used in this study was a medical grade product purchased from Dongguan Hongfeng Silicone Technology, China. The granular sodium chloride (NaCl, food grade) was purchased from Fisher Scientific with a specific gravity of 2.17. It was sieved to obtain size fractions measuring 150–300, 300–450, and 450–600 μm by using a standard sieve shaker.

Fabrication of PDMS Cell Scaffolds

The fabrication of PDMS scaffolds involves mixing liquid PDMS precursor base with a curing agent, and then pouring the mixture into a mould for curing. In this study, a certain amount of NaCl particles were put into a mould measuring 15 cm × 10 cm × 5 cm, then an NaCl preform was made by compressing NaCl particles under different pressures using a compression moulding machine [as shown in Figure 1(a)]. Figure 1(b,c) show the actual set-up and a schematic of the VARTM process, respectively. It can be seen that the NaCl preforms were placed in an open stage with a peel ply between the NaCl preform and the stage surface. Another peel ply and a highly permeable medium were placed over the NaCl pre-form, and then a vacuum bag was used to seal the NaCl pre-form within a closed domain. Two resin suction pipes were attached to the NaCl preform surface. One of them was connected to a resin trap, while the other was connected to a vacuum pump. Before resin was pumped in, vacuum was applied to the mould for 10 min for degassing to eliminate all extra air within. After degassing, the resin was introduced due to the induced pressure difference, and as it flowed in, it soaked into the NaCl preform. After the NaCl preform was completely wetted by the resin, the resin inlet pipe was clamped and then blocked off. The NaCl/PDMS composite was made and cured at room temperature for about 4–6 h. The effects of three factors (compression load, compression time, and NaCl particle size) on the properties of PDMS cell scaffolds were studied. The VARTM process parameters are given in Table I.

After the VARTM process, the moulded NaCl/PDMS composites were leached in deionized water using the set-up depicted elsewhere.[11,12] The deionized water was changed every 6 h. The samples were characterized after leaching for 5, 24, and 48 h,

Table I. VARTM Processing Parameters

Samples	Compression load (kPa)	Compression time (s)	NaCl particle size (μm)
1	0	0	300-450
2	8	10	300-450
3	16	10	300-450
4	8	60	300-450
5	8	180	300-450
6	8	60	150-300
7	8	60	450-600

respectively. In addition, to study the effect of ultrasonic oscillation on the porosity and interconnectivity of PDMS scaffolds, after leaching for 24 h, some samples were leached for one more hour under ultrasonication. The ultrasonicated, leached samples were dried in vacuum and used for characterization and application unless otherwise specified.

Morphological Characterization

The morphology of the leached PDMS scaffold was observed under an SEM S-3400N with an accelerating voltage of 15 kV. Before observation by SEM, all leached samples were fractured after immersion in liquid nitrogen and then sputter-coated with gold for 40 s.

Interconnectivity of Scaffolds

A simple method reported previously[13] was applied to test the interconnectivity of pores in the macro-porous PDMS scaffolds. First, 2-mL black ink were added to 15 mL water and stirred. Second, PDMS scaffolds were soaked, drop-wise, in alcohol. After preparation, the black ink–water mixture was dropped onto the top surface of the PDMS scaffolds. Then the sample was cut open to inspect the ink marks. The image was captured by digital camera.

Thermogravimetric Analysis

The amount of NaCl remaining inside the NaCl/PDMS composite was determined by thermogravimetric analyzer (TGA, TA instruments Q500). The samples were heated from 25 to 900°C at a rate of 20°C min^{-1}. Nitrogen was used as a flushing gas at a flow rate of 20 mL min^{-1}. The mass of each sample used for thermogravimetric analysis was about 10–12 mg.

Porosity Calculation

The porosity of the PDMS scaffold was calculated by the modified liquid replacement method.[14,15] The scaffolds were permeated with ethanol through repeated cycles of vacuum and air escape. The masses of the dry (W_{dry}) and wet (W_{wet}) samples were measured. The porosity of the scaffold, P, was determined from the mass difference between the dry and wet samples according to eq. (1):

$$P = \frac{(W_{wet} - W_{dry})/\rho_{ethanol}}{V_{app}} \times 100 \quad (1)$$

where $\rho_{ethanol}$ is the density of ethanol (0.789 g cm^{-3}), and V_{app} is the apparent volume of PDMS scaffolds (cm^3), which can be obtained by measuring the dimensions of the samples. It was assumed that the volume of pores was equal to the volume occupied by the absorbed ethanol, while the amount of ethanol absorbed by the PDMS scaffolds was negligible. The porosity data were analyzed by using Origin 7.0 software.

Water Absorption

Water absorption is an important property of cell scaffolds. The water absorption of the PDMS scaffolds was tested as follows: first, the PDMS cell scaffolds were dried in a vacuum to a constant mass (W_{dry}). Next, they were immersed in a phosphate-buffered saline (PBS) solution at 37°C and taken out at regular intervals to measure the wet mass by using a precision electronic balance. The masses of the wet samples (W_{wet}) were determined until the mass displayed did not change and the samples had therefore been completely permeated. Equation (2) was used to determine the water absorption of PDMS scaffolds as follows:

$$\text{water absorption}(\%) = \left(\frac{W_{wet} - W_{dry}}{W_{dry}}\right) \times 100 \quad (2)$$

Surface Wettability

To investigate the surface wettability (hydrophilicity or hydrophobicity) of the scaffolds, the water contact angle of solid PDMS, and PDMS scaffolds with different pore sizes, were measured by a video contact angle system (SL200B, China). The deionized water droplet volume was set to 30 μL. The surface contact angle was measured after the water drop was stable on the surface. Three samples of each type were tested and the average value was reported with its standard deviation.

Mechanical Properties

The leached PDMS samples were cut into pieces with a diameter of 13 cm and tested, in compression, on an electronic universal testing instrument (MTS, CMT6104). The compression test parameters followed those in ISO 815:1991 (Standard Test Method for Rubber, Vulcanized or Thermoplastic). A constant crosshead rate of 2 mm min^{-1} was used until a 50% deformation was reached in the thickness direction. Five samples were measured for each type of samples. The compressive modulus (E) was estimated from the initial slope of the linear region of the stress–strain curve. The compressive strength at a 50% deformation was determined.

In Vitro Cell Seeding and Culture

Osteoblasts were harvested from infant SD rats, which were expanded in culture medium consisting of low-glucose DMEM supplemented with 10% fetal bovine serum (FBS) until reaching 80% confluence. Cells were seeded onto the PDMS scaffolds (samples 4, 6, and 7) measuring 1 cm × 1 cm at 10^5 cells cm^{-2}, with an additional 3 mL of the appropriate medium added into each well afterward. The culture was maintained in a cell culture incubator at 95% humidity and 5% CO_2 at 37°C. The culture medium was replaced every other day. At days 1, 3, and 5, scaffolds were collected and characterized for cytotoxicity analysis.

Cytotoxicity Study of Cells on the Scaffolds

For cytotoxicity testing, osteoblasts from infant SD rats were seeded at a cell density of 10^5 cells/well on the PDMS scaffolds (samples 4, 6, and 7) placed in the 24-wells. The viability of seeded cells on the PDMS scaffold was measured after 1, 3, and 5 days by MTT assay. The scaffolds, with their attached cells, were incubated in a mixture of 360 μL of phosphate buffer saline (PBS) and 40 μL MTT solution (5 mg mL^{-1} in PBS) for 4 h at 37°C in a 5% CO_2 atmosphere. The intense red colored formazan derivatives formed were dissolved in 400 μL dimethyl sulfoxide for 15 min and the absorbance was measured at 490 nm using a plate reader.

Cell Attachment

The morphology of the adherent cells on the PDMS scaffold was examined by SEM. To prepare the samples for SEM analysis, the samples were soaked in 2.5% (v/v) glutaraldehyde for 1 h at room temperature and washed in PBS solution to remove any excess glutaraldehyde. The fixed cells were dehydrated in gradient ethanol starting from 50, 60, 70, 80, 90% and finally

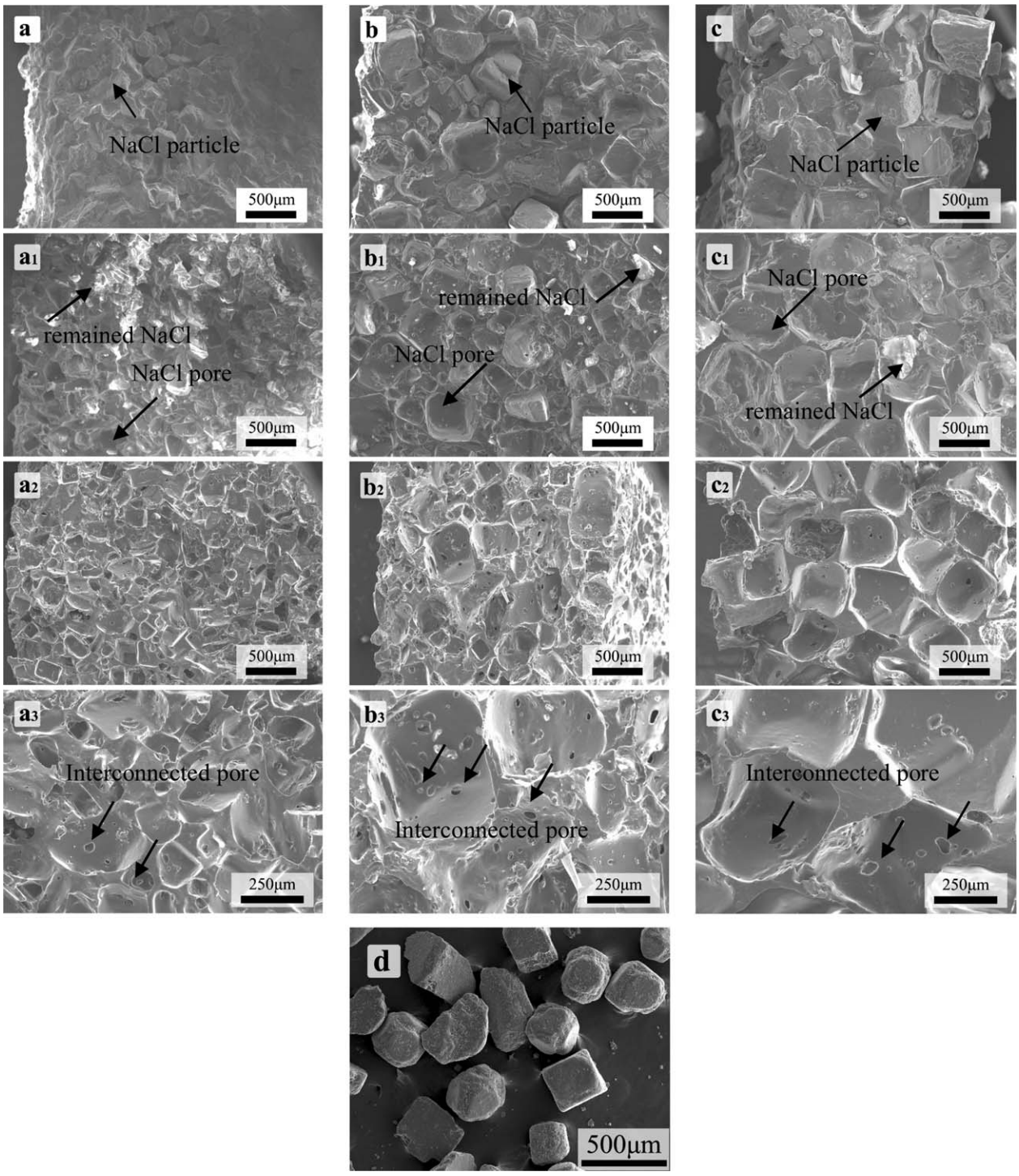

Figure 2. SEM images of PDMS/NaCl samples with different NaCl particle size after leaching for 0 h (a–c), 24 h (a1–c1), and 24 h with ultrasonication for 1 h (a2–c2). (a3–c3) are the magnified versions of (a2–c2), respectively, and (d) SEM images of NaCl.

100% for 10 min each. The dehydrated scaffolds were dried and observed by SEM.

RESULTS AND DISCUSSION

Morphology of PDMS Scaffolds

The PDMS/NaCl composites were fabricated, leached by deionized water, fractured, and then examined by SEM as described previously. Figure 2 shows the representative micrographs of PDMS/NaCl samples with various NaCl particle sizes: 150–300 μm [Figure 2(a–a3)], 300–450 μm [Figure 2(b–b3)], and 450–600 μm [Figure 2(c–c3)] after leaching for different periods of time. All NaCl preforms were processed at a compression load of 8 kPa for 60 s. Before leaching, the PDMS/NaCl samples showed solid NaCl particles with no visible pores [Figure 2(a–

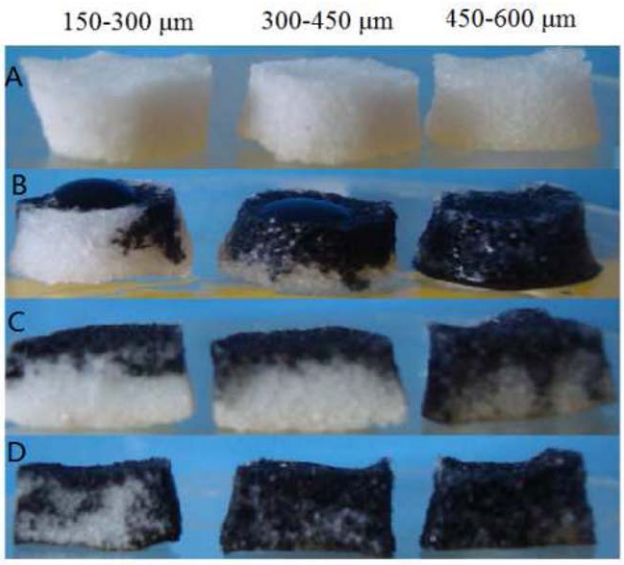

Figure 3. The interconnectivity testing of PDMS scaffolds with different pore sizes. [The PDMS scaffolds (A), ink transfusion (B), and photos of the ink seepage created by 0.4 mL (C) and 0.8 mL (D) ink]. [Color figure can be viewed in the online issue, which is available at wileyonlinelibrary.com.]

c)]. From Figure 2(a1–c1), it can be seen that, after leaching for 24 h, most solid NaCl particles dissolved, which left many pores. However, a few NaCl porogens remained (indicated by arrows). This might be attributed to some NaCl porogens being trapped in the PDMS phase, which could not be removed. From Figure 2(a2–c2), it can be found that, by applying an additional hour of leaching under ultrasonication, there were no obvious NaCl particles remaining in the PDMS surface. In addition, to observe the surface features of the pores clearly, the magnified images are shown in Figure 2(a3–c3). It was interesting to see that many of the smaller pores could be observed within larger NaCl pores. This was probably because some ultra-thin-walls between the pores of the leached PDMS sample were broken during ultrasonication, which resulted in more connected pores. These connected pores further increased the interconnectivity of PDMS scaffolds, which helped to dissolve more NaCl particles. This indicated that ultrasound could improve the porosity and interconnectivity of PDMS scaffolds. This would be discussed and demonstrated further in the section covering the TGA results. For comparison, SEM images of NaCl particles are provided in Figure 2(d). In all samples, the pore sizes of 150–300, 300–450, and 450–600 μm matched those of the NaCl particles, which confirmed that the pores were formed by porogen leaching. Moreover, the shape of formed pores inside the PDMS scaffold is the same as those of the original NaCl particles. This indicated that the NaCl particle will retain its shape and will not be crushed during processing. Other research[16–18] showed that the predominant pore size in bone tissues had the same ranges as those obtained in this study.

Interconnectivity of PDMS Scaffolds

Figure 3 shows a digital image of the PDMS scaffolds, the processing by ink transfusion, and the ink seepage created by 0.4 and 0.8 mL of ink. For interconnectivity tests on PDMS scaffolds with different pore sizes, all NaCl preforms were measured at a compression load of 8 kPa and after a compression time of 60 s. In Figure 3(b), it can be seen that the larger the pore sizes in the PDMS scaffold, the quicker the ink permeated, which indicated the better penetration ability and interconnectivity thereof. The results of ink seepage [Figure 3(c,d)] showed that the PDMS scaffolds with pore sizes of 300–450 μm and 450–600 μm had good interconnectivity. This indicated that the PDMS/NaCl blend was a dual-phase continuous structure before leaching. After leaching, well interconnected pores were formed in the PDMS scaffold. However, the interconnectivity of the PDMS scaffold with pore sizes of 150–300 μm was poor compared with those of scaffolds with larger pore sizes. This might have been because the smaller the size of NaCl particles, the less the contact area between them, which resulted in poor interconnectivity. These results implied that the PDMS scaffold with good interconnectivity could be fabricated by choosing a suitable size of NaCl porogen.

Residual NaCl Contents in PDMS Scaffolds

Figure 4(a) shows the TGA curves of solid PDMS and PDMS/NaCl composites (sample 4) with different leaching times. As shown in Figure 4(a), when the temperature exceeded 900°C, the residual mass ratio of solid PDMS was ~71%. Most of these char residues were in the form of amorphous silica due to the pyrolytic degradation of silicon.[19] For PDMS/NaCl composites, the char residual weight was the sum of silica and remaining NaCl particles. The mass ratio of the pyrolytic degradation product of solid PDMS was a constant when heated to 900°C. The content of residual NaCl in the PDMS/NaCl composites, after leaching, can be calculated by eq. (3):

$$r_{\mathrm{NaCl}}\% = (r_{\mathrm{PDMS/NaCl}} - r_{\mathrm{PDMS}} \times C_{\mathrm{PDMS}}) \times 100 \quad (3)$$

where r_{PDMS} and $r_{\mathrm{PDMS/NaCl}}$ are the mass ratios of the remaining products of PDMS/NaCl composites and solid PDMS heated above 900°C, respectively (both of them can be obtained from TGA curves [Figure 4(a)], and C_{PDMS} is the content of PDMS (wt %) in the PDMS/NaCl composite (27.9% in Sample 6).

Figure 4(b) shows the concentration of residual NaCl (wt %) in the PDMS/NaCl composites (sample 4) after leaching for different periods of time. From Figure 4(b), it can be found that there was only 18.7 wt % NaCl particles remaining after leaching for 5 h. This meant that the most of NaCl particles in the PDMS/NaCl composites were leached out during the first 5 h. The contents of residual NaCl in the samples leached for 24 and 48 h were similar, *i.e.* 9.0 and 8.6 wt %, respectively. This indicated that, after leaching for 24 h, increasing the leaching time had minimal, to no, effect on the removal of NaCl particles. This might have been due to some NaCl particles being trapped within the PDMS phase. However, the mass ratio of the residual NaCl was reduced to 4.8 wt % when the samples were leached for a further 1 h under ultrasound. This might have been attributed to breakage of the thin-walls between pores during ultrasonication, resulting in more NaCl particles leaching out. Thus, the TGA results were consistent with those of SEM results discussed above.

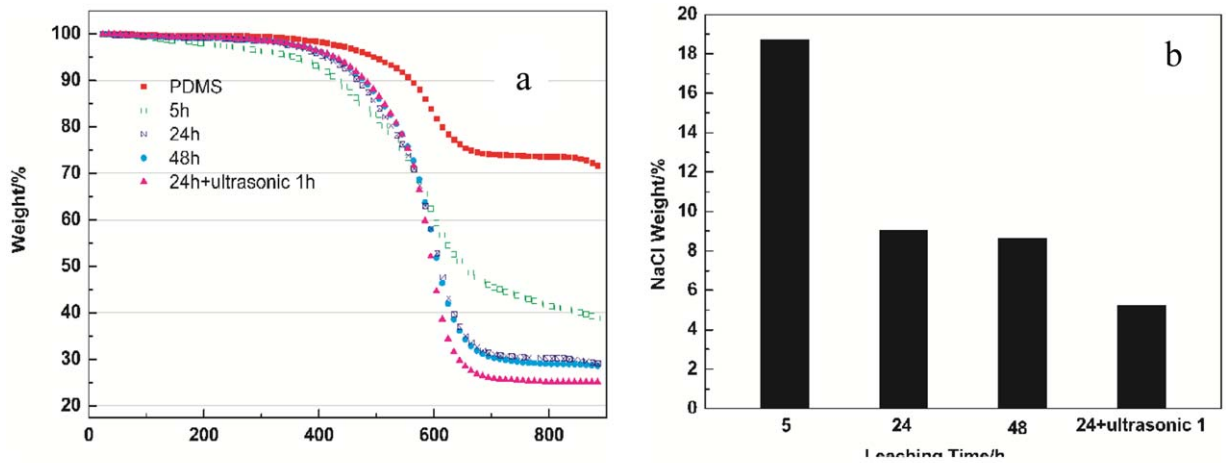

Figure 4. (a) TGA curves of solid PDMS and the PDMS/NaCl blend composites after leaching different times *versus* temperature. (b) The residual NaCl content (wt %) in the PDMS/NaCl blend composites after leaching different times. The NaCl particle size was 150–300 μm. [Color figure can be viewed in the online issue, which is available at wileyonlinelibrary.com.]

Figure 5(a,b) show TGA curves and the residual NaCl content for PDMS scaffolds (samples 4, 6, and 7) with different pore sizes. From Figure 5(b), it can be seen that the residual NaCl content of a PDMS scaffold with pore sizes between 150 and 300 μm was larger compared with that of a PDMS scaffold with pore sizes of 300–450 μm, and 450–600 μm. This was because the larger the NaCl particle size, the larger the pores formed, the better their interconnectivity, and the lower the remaining NaCl content. Therefore, better interconnectivity benefitted lower residual NaCl content development.

Porosity and Water Absorption of Prepared PDMS Scaffolds

The porosity and water absorption of scaffolds are important factors for cell culture, since scaffolds should provide sufficient space for cell adhesion and growth, and for culture solution absorption and transfer. The porosity and water absorption of prepared PDMS scaffolds formed with various NaCl particle sizes, compression loads, and compression times are shown in Figure 6(a–c). Figure 6(a) indicates that the porosity of PDMS scaffolds decreased slightly with increasing NaCl particle size under a compression load of 8 kPa and a compression time of 60 s. This could be attributed to the compactness of the NaCl preform. When the compression load and compression time were constant, the smaller the NaCl particle size, the higher the compactness of NaCl preform, resulting in less void space into which to inject the liquid PDMS precursor [as shown in Figure 6(d)], and the higher the porosity. Moreover, the water absorption decreased with increasing NaCl particle size and decreasing scaffold porosity. This was because the PDMS matrix was hydrophobic, and its ability to absorb water would therefore be negligible. The void space in the scaffold was the main factor affecting water absorption, since scaffolds with higher porosity had more water storage space. This result was in agreement with the literature.[20–22] As seen in Figure 6(b,c), the porosity and water absorption of scaffolds were almost the same when the NaCl preforms were prepared under different compression loads and compression times, which suggested that there was no significant effect exerted by the processing parameters on the

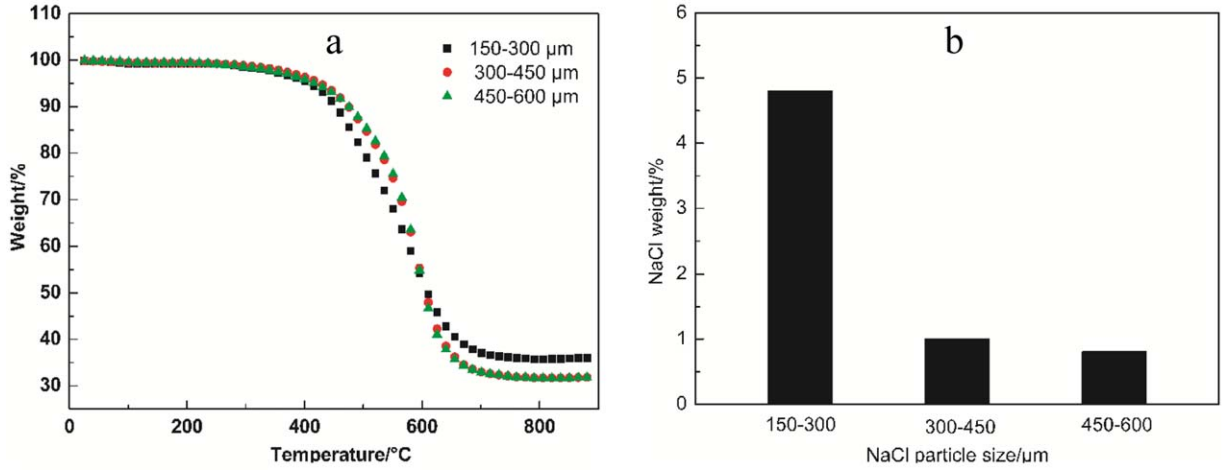

Figure 5. TGA curves (a) and the residual NaCl content (b) of PDMS scaffold with different pore size. [Color figure can be viewed in the online issue, which is available at wileyonlinelibrary.com.]

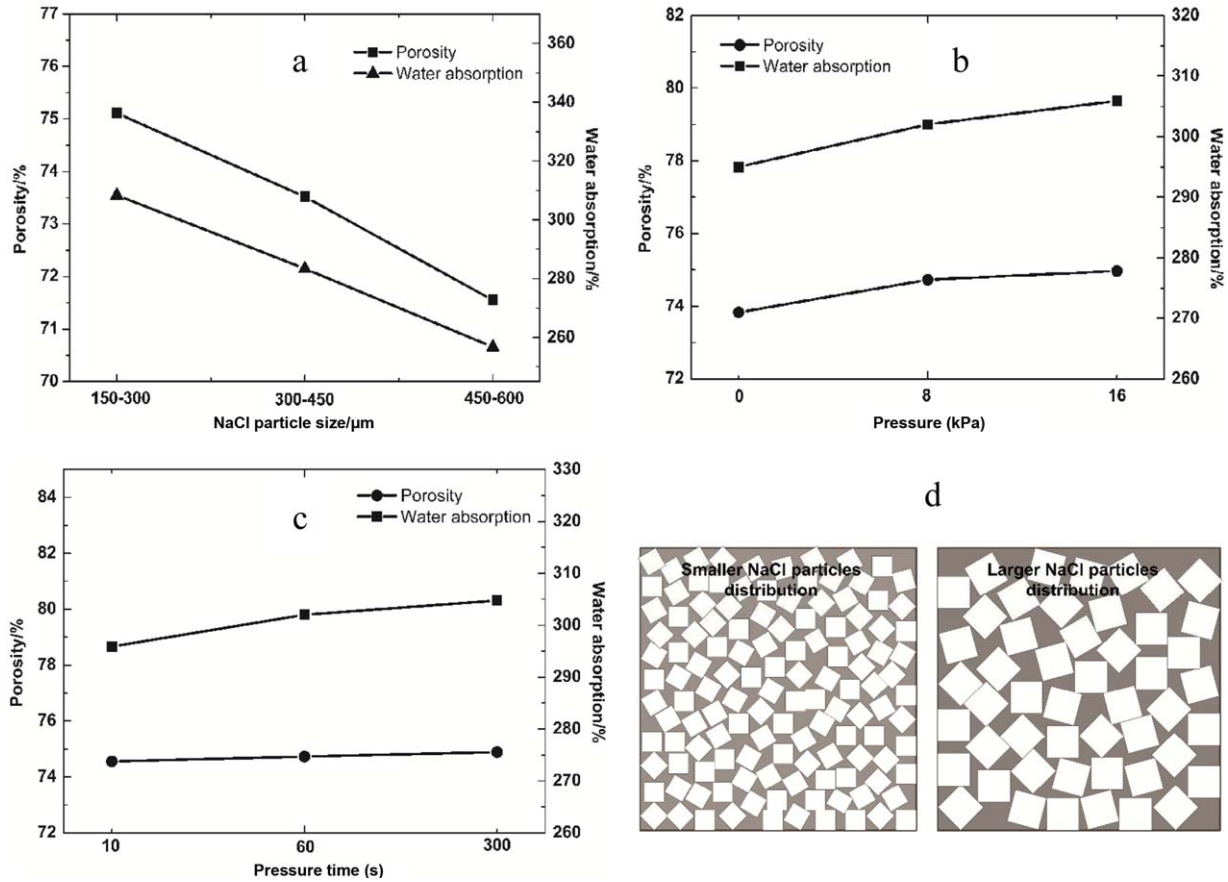

Figure 6. Porosity and water absorption of prepared PDMS scaffolds with different NaCl particle sizes (a), compression load (b), compression time (c), and the distribution schematic of NaCl particles with different sizes (d). [Color figure can be viewed in the online issue, which is available at wileyonlinelibrary.com.]

porosity and water absorption. The porosity and water absorption mostly depended on the size of the NaCl particles.

Surface Wettability of PDMS Scaffolds

Wettability is an important property of a solid surface. It is governed by the surface chemical composition and geometrical microstructures (e.g., surface roughness, pore size, and porosity). Figure 7 shows the water contact angles for solid PDMS and leached PDMS scaffolds (samples 4, 6, and 7) with different pore sizes. The data from the water contact angle measurements implied a hydrophobic surface characteristic of solid PDMS. All PDMS scaffolds, with various pore sizes of 150–300, 300–450, and 450–600 μm, had average contact angles of 95.4°, 115.8°, 114.9°, and 109°, respectively. The water contact angles for all of the PDMS scaffolds were higher than that of solid PDMS due

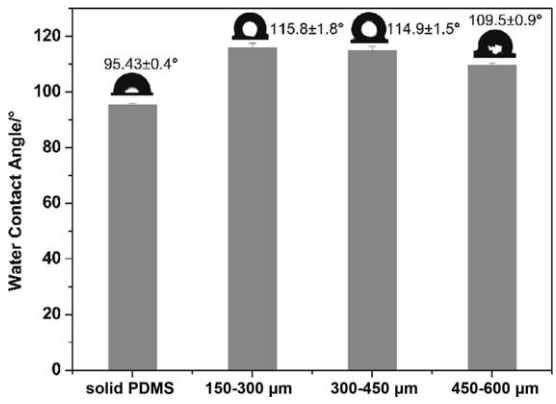

Figure 7. Water contact angles of solid PDMS and PDMS scaffolds with various NaCl particle sizes.

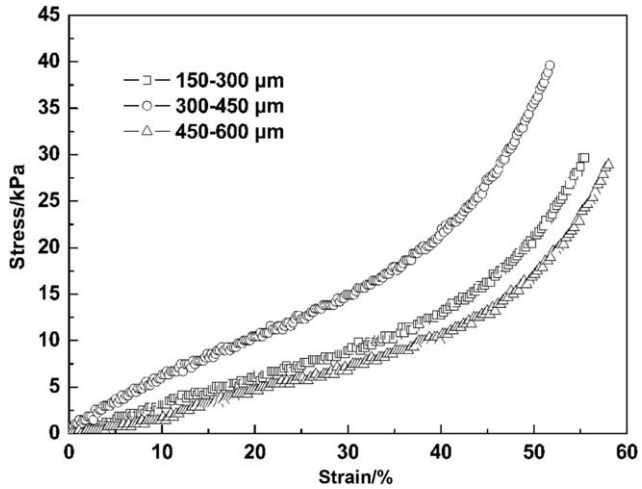

Figure 8. Stress–strain curves for PDMS scaffolds with different pore sizes.

Table II. Compressive Modulus and Compressive Strength of PDMS Scaffolds with Different Pore Sizes

Pore size (μm)	Compressive modulus (kPa)	Compressive strength (kPa)
150-300	31.86	21.10
300-450	40.32	35.21
450-600	31.15	17.56

to the effects of the micro-porous structure and higher surface roughness. The water contact angle of PDMS scaffolds increased with decreasing pore size, which was in agreement with other results.[23]

Mechanical Properties of PDMS Scaffolds

The compressive modulus is another important property of a cell scaffold. Figure 8 shows the stress–strain curves of PDMS scaffolds (samples 4, 6, and 7) with different pore sizes. The values of compressive modulus and compressive strength obtained from such stress–strain curves are shown in Table II. PDMS scaffolds with a pore size of 300–450 μm had the greatest compressive modulus and compressive strength. The reason was that both smaller and larger NaCl particle sizes would lead to a higher porosity and a better interconnectivity respectively, which resulted in lower mechanical properties. This suggested that the porosity, pore interconnectivity, and structure exerted significant influence on the mechanical properties of such scaffolds. In addition, the compressive modulus of fabricated PDMS scaffolds ranged from 30 to 40 kPa, which indicate that PDMS scaffolds have good flexibility and could offer potential in meeting the mechanical property requirements for soft tissue, such as skin, blood vessel, tendon, ligament, etc.

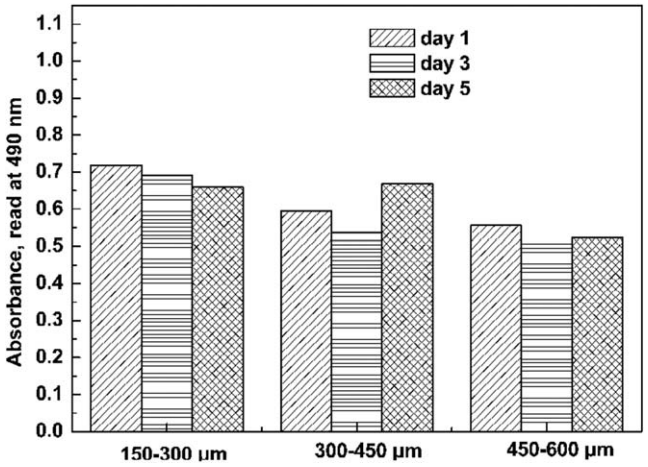

Figure 9. MTT analysis of metabolic activity of osteoblast from infant SD rats seeded on PDMS scaffolds with different pore size at 1, 3, and 5 days.

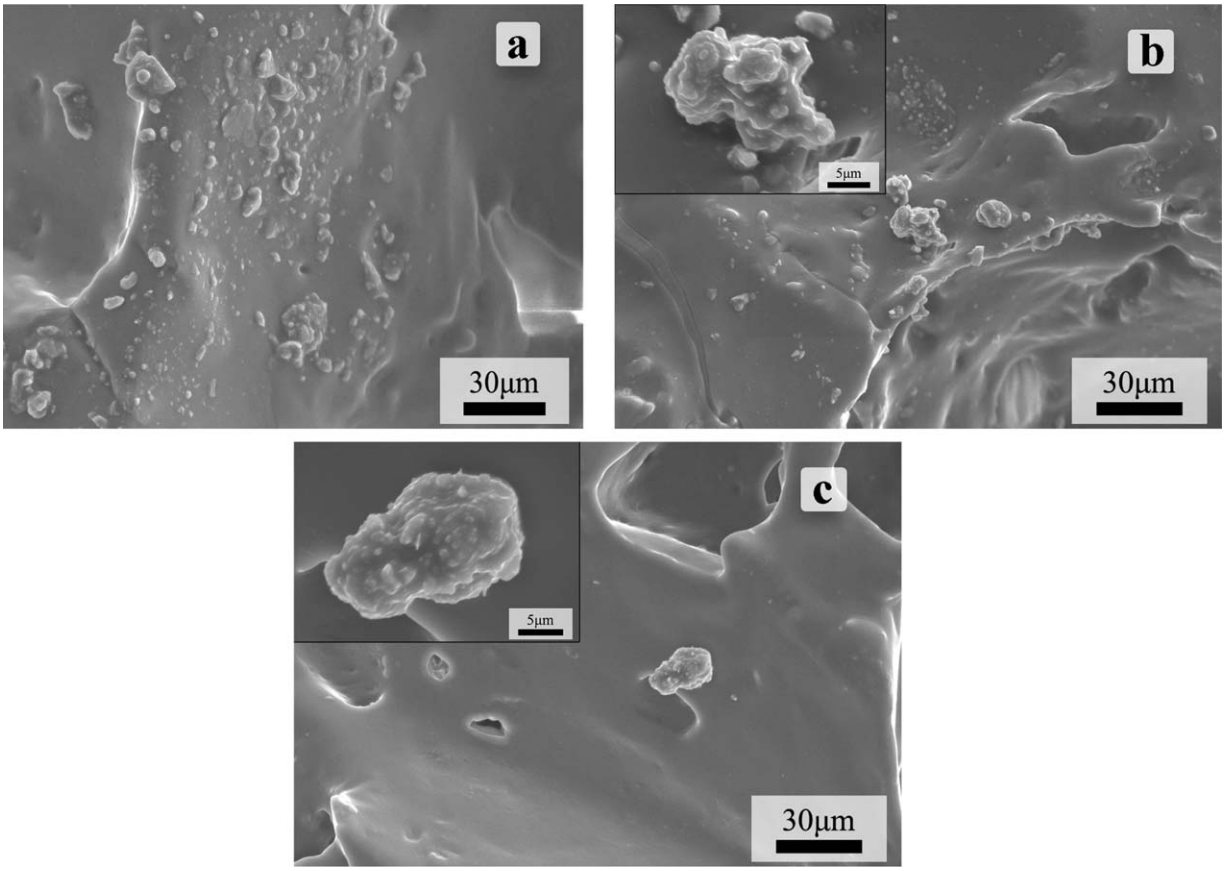

Figure 10. SEM graphs of osteoblast from infant SD rats after 24 h incubation on PDMS scaffolds with different pore sizes: 150–300 μm (a), 300–450 μm (b), and 450–600 μm (c).

Cytotoxicity Study of Cells on the Scaffolds

The metabolic activity of osteoblasts, from infant SD rats, seeded on PDMS scaffolds with different pore sizes was analyzed using an MTT assay. The MTT assay is based on the reduction of yellow tetrazolium salt to purple formazan crystals by dehydrogenases secreted by the mitochondria of metabolically active cells. The amount of purple formazan crystals formed is proportional to the number of viable cells.[24] As shown in Figure 9, after 1, 3, and 5 days of incubation, the number of cells in the PDMS scaffolds was not significantly decreased and the cell survival rate was ~70%. This indicated that the PDMS scaffold had no obvious harmful effects on the growth of osteoblasts. The PDMS scaffolds prepared had no toxicity and would be a potential matrix for cell culture.

The morphology of the cells on PDMS scaffolds with different pore sizes was observed under SEM. The cell morphologies on all PDMS scaffolds were found to have been similar [Figure 10(a–c)] and maintained a round shape after 24-h incubation. Although the cells were attached to the scaffold surface, no pseudopodial protrusion was observed. PDMS scaffolds had a hydrophobic surface, as mentioned, which made it difficult for cells to stretch over the surface of the scaffold. Therefore, how to improve the hydrophilicity of the PDMS scaffolds prepared in this study would be worthy of further research.

CONCLUSION

In this study, 3D PDMS cell scaffolds with high porosity and water absorption were produced by combining VARTM and particle leaching technologies. The morphology, porosity, water absorption, interconnectivity, and wettability of PDMS scaffolds, as well as their mechanical properties and biocompatibility were investigated. The test results showed that the smaller the size of the NaCl particles, the higher the porosity and water absorption of the PDMS cell scaffolds. The highest porosity and water absorption of PDMS cell scaffolds reached 76 and 302%, respectively. The interconnectivity of PDMS cell scaffolds increased with increasing of NaCl particle size. The compressive modulus and compressive strength of PDMS scaffolds with pore sizes of 300–450 μm were larger than scaffolds with pore sizes of 150–300 μm and 450–600 μm. Also, the MTT assay results indicated that these PDMS scaffolds had no harmful effects on the growth of osteoblasts from infant SD rats, showing a satisfactory biocompatibility therewith.

ACKNOWLEDGMENTS

The authors thank The National Natural Science Foundation of China (Grant No. 51303027, 11572290), China Postdoctoral Science Foundation (Grant No. 2014M560525), the University Scientific Research Foundation of Fujian (Grant No. JK2014030), and the Fujian Undergraduate Training Programs for Innovation and Entrepreneurship (Grant No. 201410388065) for their financial supports.

REFERENCES

1. Meyvantsson, I.; Beebe, D. *J. Annu. Rev. Anal. Chem.* **2008**, *1*, 423.
2. Griffith, L. G.; Naughton, G. *Science* **2002**, *295*, 1009.
3. Borenstein, J. T.; Weinberg, E. J.; Orrick, B. K.; Sundback, C.; Kaazempur-Mofrad, M. R.; Vacanti, J. P. *Tissue Eng.* **2007**, *13*, 1837.
4. Pedraza, E.; Brady, A. C.; Fraker, C. A.; Stabler, C. L. *J. Biomater. Sci. Polym. E.* **2012**, *24*, 1041.
5. Hassler, C.; Boretius, T.; Stieglitz, T. *J. Polym. Sci. Part B: Polym. Phys.* **2011**, *49*, 18.
6. Halldorsson, S.; Lucumi, E.; Gomez-Sjoberg, R.; Fleming, R. *Biosens. Bioelectron.* **2015**, *63*, 218.
7. Kang, M. K.; Lee, W. I.; Hahn, H. T. *Compos. A* **2001**, *32*, 1553.
8. Paglicawan, M. A.; Kin, B. S.; Blessie-Basilia, A. B.; Emolaga, C. S.; Marasigan, D. D.; Maglalang, P. E. C. *Precis. Eng.* **2014**, *1*, 241.
9. Matsuzaki, R.; Kobayashi, S. J.; Todoroki, A. *Compos. A* **2013**, *45*, 79.
10. Simacek, P.; Eksik, O.; Heider, D. *Compos. A* **2012**, *43*, 370.
11. Kramschuster, A.; Turng, L. S. *J. Biomed. Mater. Res. B* **2010**, *92B*, 366.
12. Cui, Z.; Nelson, B.; Peng, Y.; Li, K.; Pilla, S.; Li, W. J.; Turng, L. S.; Shen, C. *Mater. Sci. Eng. C* **2012**, *32*, 1674.
13. Gong, X.; Tang, C.; Zhang, Y.; Wong, C. T. *J. Appl. Polym. Sci.* **2012**, *125*, 571.
14. Gong, X.; Tang, C.; Wong, C. T.; Lu, W.; Zhang, Y.; Lam, W. M.; Wu, S. P.; Liu, J. *e-Polymers* **2010**, *1*, 1264.
15. Yang, Y.; Zhao, J.; Zhao, Y.; Wen, L.; Yuan, X.; Fan, B. *J. Appl. Polym. Sci.* **2008**, *109*, 1232.
16. Oh, S. H.; Park, I. K.; Kim, J. M.; Lee, J. H. *Biomaterials* **2007**, *28*, 1664.
17. Beletskii, B. I.; Sh, D.; Mastryukova, E.; Vlasova, B. *Glass Ceram.* **2003**, *60*, 270.
18. Karageorgiou, V.; Kaplan, D. *Biomaterials* **2005**, *26*, 5474.
19. Lewicki, J. P.; Worsley, M. A.; Albo, R. L. F. *Polym. Degrad. Stabil.* **2014**, *102*, 25.
20. Wen, P.; Gao, J.; Zhang, Y.; Li, X.; Long, Y.; Wu, X. *J. Biomater. Sci.* **2011**, *22*, 19.
21. Chang, C. P.; Hsu, C. C. *Mater. Sci. Eng. A* **2006**, *433*, 100.
22. Cui, Z.; Zhao, H.; Peng, Y.; Han, J.; Turng, L. S.; Shen, C. *J. Biobased Mater. Bioenergy* **2014**, *8*, 281.
23. Li, X.; Fan, X.; Brandani, S. *Chem. Eng. Sci.* **2014**, *117*, 137.
24. Thadavirul, N.; Pavasant, P.; Supaphol, P. *J. Biomed. Mater. Res. A* **2014**, *102A*, 3379.